Journal of Engineering Mathematics **24**: 311–321, 1990.

Computations on flow past an inclined flat plate of finite length

F.T. SMITH and S.C.R. DENNIS*

*Department of Mathematics, University College London, Gower Street, London WC1E 6BT, UK; *permanent address: Applied Mathematics Dept., University of W. Ontario, London, Ontario, Canada*

Received 9 November 1989; accepted in revised form 22 March 1990

Abstract. This paper deals with the numerical solution of the Navier-Stokes equations for the steady planar laminar flow of an incompressible viscous fluid past a finite flat plane, at various angles of incidence to an oncoming uniform stream at infinity and at various Reynolds numbers Re.

1. Introduction

Our concern is with the numerical solution of the Navier-Stokes equations for the steady planar laminar flow of an incompressible viscous fluid past a finite flat plate, at various angles of incidence to an oncoming uniform stream at infinity and at various Reynolds numbers Re. This fundamental physical problem, which also has considerable technological interest, seems challenging and difficult computationally for several reasons, in particular due to the sharp leading and trailing edges and their associated singularities, the farfield conditions, and the lack of symmetry, at least for the most interesting range $0 < \alpha < \pi/2$ of the angle of incidence α. As far as we know there are no accurate computations for this motion reported in the literature. This is in contrast with the special cases of symmetrical geometry where $\alpha = 0$ (Dennis and Dunwoody [3], Dennis [2] and others) or $\alpha = \pi/2$ (Hudson and Dennis [7]), although we note that there are numerous computations of nonsymmetric smooth airfoil flows involving various degrees of approximation, as reviewed by Smith [10] and Vatsa and Verdon [14] for example, and also numerous experimental studies as mentioned in the above references. The problem area is of physical interest because of its possible insight into leading-edge and trailing-edge separation or stall (e.g. see Mehta [9], Stewartson, Smith and Kaups [13], Smith [11]), particularly at relatively small angles α, and into recirculating-eddy formation downstream. Again, there is the question of comparing with asymptotic theory for nonzero α, given that the comparison in the aligned case $\alpha = 0$ is remarkably close as regards the drag (Jobe and Burgraf [8]; see also Veldman and Van de Vooren [15]).

An issue of some significance considered here, apart from the intrinsic interest of the flow properties, is the computational treatment of the flow solution near the leading and trailing edges. Specifically, we investigate the accuracy, or its limitations, achieved by using a relatively straightforward "geometrical" method locally to allow for the singularities at the edges, within a vorticity-streamfunction formulation (cf. Hudson and Dennis [7]). This is with the aim of determining whether such a local method is sufficiently reliable at various α values and Reynolds numbers or whether an alternative, possibly more sophisticated, treatment is essential. Our earlier study (Smith and Dennis [12]) of an injection problem shows that the method does work reasonably well in at least one context, which tends to point perhaps to some optimism in the application to other contexts also, such as the present nonsymmetric plate motions.

Attention is focussed, then, on the flow response near the plate in particular, when the geometrical method, which skirts around the leading and trailing edges, is adopted. For that reason we do not go to great lengths in this work to ensure that the outer, freestream, conditions are captured accurately as infinity conditions, although generally it turns out that, despite the importance of these conditions here and in previous computations, the distortion due to the outer boundary conditions chosen here appears to be not excessive on the plate in the parameter ranges addressed, certainly in qualitative terms. A complementary study is being considered, however, to tackle the farfield constraints more accurately for flow past inclined ellipses; the inclined flat plate will also be considered as a limiting, but rather more difficult, case.

The computational approach is described in Sec. 2 below. Its main aspects are the use of extended finite differences as in Dennis [1], Dennis and Hudson [4] and subsequent works, the geometrical treatment of the local leading- and trailing-edge flows, and the nominal second-order accuracy of the overall scheme. The results are presented in Sec. 3, along with comparisons and checks, and further comments are made in Sec. 4. It is found that while the simple treatment of the edge singularities works less well than in Smith and Dennis [12] the resulting distortion of the wall-shear solution along the plate is confined fairly locally, near the edges, and it reduces consistently with refinements of the grid. Results are presented for angles of incidence $\alpha = 0$, $\pi/4$, $\pi/2$ with Reynolds numbers $\mathrm{Re} \equiv u_\infty l/\nu$ up to 50. Here u_∞ is the freestream speed, the plate length is $2l$ and ν is the kinematic viscosity of the incompressible fluid. Clearly a more refined treatment of the edges would be desirable, but progress in this respect has been slow in the literature; it presents a quite difficult problem.

2. The computational approach

We adopt a cartesian coordinate system aligned with the plate (Fig. 1), so that the continuity and Navier-Stokes equations may be converted to the form

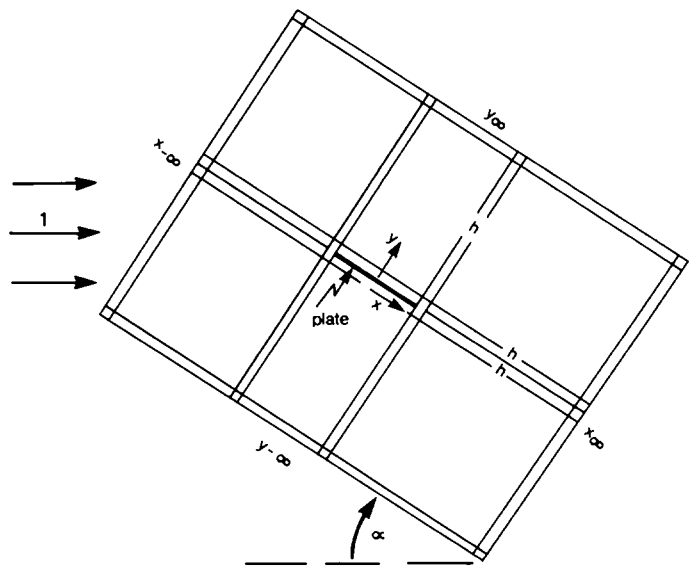

Fig. 1. Sketch of the arrangement of the computational grid, with mesh size h, for angles of incidence α ($0 \leq \alpha \leq \pi/2$).

$$(\partial\psi/\partial y)(\partial\zeta/\partial x) - (\partial\psi/\partial x)(\partial\zeta/\partial y) = \mathrm{Re}^{-1}\nabla^2\zeta\,, \tag{2.1a}$$

$$\zeta = -\nabla^2\psi \tag{2.1b}$$

controlling $\psi(x, y)$, $\zeta(x, y)$, along with the boundary conditions

$$(\partial\psi/\partial y, -\partial\psi/\partial x) \to (\cos\alpha, \sin\alpha) \quad \text{as } x^2 + y^2 \to \infty\,, \tag{2.1c}$$

$$\psi_0,\ \partial\psi/\partial y = 0 \quad \text{at } y = 0 \text{ for } -1 < x < 1\,. \tag{2.1d, e}$$

Here α is the angle of incidence, taken such that $0 \leqslant \alpha \leqslant \pi/2$, while the velocity components u, v and the lengths x, y have been nondimensionalized with respect to u_∞, l, in turn, ψ is the corresponding stream function satisfying $u = \partial\psi/\partial y$, $v = -\partial\psi/\partial x$ and ζ is the normalized vorticity. Also, the operator $\nabla^2 \equiv \partial^2/\partial x^2 + \partial^2/\partial y^2$.

In the computational approach the second-order scheme of Dennis [1], Dennis and Hudson [4], Dennis and Smith [6] and subsequent papers is applied for the discretization of the governing equations (2.1a, b). The range of numerical integration $x_{-\infty} \leqslant x \leqslant x_\infty$, $y_{-\infty} \leqslant y \leqslant y_\infty$ is spanned by a uniform rectangular grid having M, N lines parallel to the x, y axes respectively, with the constants $x_{\pm\infty}$, $y_{\pm\infty}$ here replacing $\pm\infty$ in effect. Thus taking $x_{-\infty} = -x_\infty < 0$, $y_{-\infty} = -y_\infty < 0$ we have $x_\infty = (N-1)h/2$, $y_\infty = (M-1)h/2$ for a given mesh width h in both the x, y directions. The mesh is chosen so that two meshpoints coincide with the leading and trailing edges. Then the augmented central-difference approximation

$$\begin{aligned}&[1 - \mathrm{Re}\,hu_0/2 + (\mathrm{Re}\,hu_0)^2/8]\zeta_1 + [1 - \mathrm{Re}\,hv_0/2 + (\mathrm{Re}\,hv_0)^2/8]\zeta_2\\ &\quad + [1 + \mathrm{Re}\,hu_0/2 + (\mathrm{Re}\,hu_0)^2/8]\zeta_3 + [1 + \mathrm{Re}\,hv_0/2 + (\mathrm{Re}\,hv_0)^2/8]\zeta_4\\ &= [4 + (\mathrm{Re}\,h)^2(u_0^2 + v_0^2)/4]\zeta_0\end{aligned} \tag{2.2}$$

is made for (2.1a), whereas (2.1b) is replaced by the standard central differencing

$$-h^2\zeta_0 = \psi_1 + \psi_2 + \psi_3 + \psi_4 - 4\psi_0\,. \tag{2.3}$$

In (2.2), (2.3) the subscripts 0, 1, 2, 3, 4 stand for evaluation at the points (x_0, y_0), $(x_0 + h, y_0)$, $(x_0, y_0 + h)$, $(x_0 - h, y_0)$, $(x_0, y_0 - h)$ in turn, where (x_0, y_0) is a typical internal gridpoint, i.e. excluding the outer boundaries $x = x_{\pm\infty}$, $y = y_{\pm\infty}$, the plate $y = 0$ for $0 \leqslant x \leqslant 1$, and two special points near $x = \pm 1$: see also below. Further, $u_0 = (\psi_2 - \psi_4)/2h$ and $v_0 = (\psi_3 - \psi_1)/2h$ employ the usual central-difference approximations. The main, and non-standard, feature here is the inclusion of the extra terms involving $(\mathrm{Re}\,h)^2$ in (2.2). These serve to ensure (assuming $\mathrm{Re}\,h$ sufficiently small) that diagonal dominance is maintained in the difference equations at all Reynolds numbers, together with second-order accuracy, as opposed to the standard central-difference schemes which lose diagonal dominance at higher Reynolds numbers, as described in detail in the last-named papers. Of course, it can be argued that in the approximation (2.2), the terms involving the square of the Reynolds number create artificial viscosity, as it is sometimes called. That may be true in some senses, but at least the balance of these additional terms is second-order accurate as opposed to the raw (i.e. uncorrected first-order accurate) upwind schemes. Moreover, numerous examples can be found in which (2.2) gives manifestly better results than the central-difference approximation, which corresponds to suppressing the terms in Re^2 in

(2.2). Just the same, it should be mentioned that if Re h is O(1) the terms in h^2 in (2.2) are of the same order as the terms in h and, also, neglected terms of order $\mathrm{Re}^2 h^4$ are then as important as terms of order h^2. Approximations for high Re must therefore be viewed with great care. However, it has been shown (Dennis and Hudson [5]) that the terms in Re^2 in (2.2) are embedded in an h^4-accurate scheme (although with slightly different coefficients of 1/12 and 1/6, respectively, on the left and right-hand sides of (2.2)). If one takes into account these various features, it seems worthwhile to employ such a scheme, with its obvious advantage of an associated diagonally dominant matrix.

A second noteworthy feature concerns the treatment of the solution near the leading and trailing edges $(x, y) = (-1, 0)$, $(1, 0)$, specifically at the two special points $(x, y) = (-1 - h, 0)$, $(1 + h, 0)$. There the use of (2.2) would bring in the value of the vorticity ζ at $(-1, 0)$ or $(1, 0)$ but in fact ζ is known to be singular at these two points since it behaves locally like distance to the power $-1/2$, e.g. for the case $\alpha = 0$, near the leading and trailing edges. To circumvent this difficulty simply the differencing of (2.1a) at $(-1 - h, 0)$ and $(1 + h, 0)$ is applied in the skewed directions $y \pm x$ rather than the directions y, x as in (2.2), thus yielding a five-point formula between the solution values at $(-1 - h, 0)$, $(-1, \pm h)$, $(-1 - 2h, \pm h)$ and similarly at $(1 + h, 0)$, $(1, \pm h)$, $(1 + 2h, \pm h)$. That preserves the nominal second-order accuracy of the method. The skewing is not applied to (2.1b) at the two special points, however, since ψ and its first derivatives are finite at the leading and trailing edges and so it seems reasonable to still use (2.3) there.

The boundary conditions on the plate are represented as follows. First, from (2.1d) we have

$$\psi = 0 \quad \text{for points } y = 0, -1 + h \leqslant x \leqslant 1 - h\,, \tag{2.4}$$

and local analysis allows ψ to be set to zero at $(x, y) = (-1, 0)$, $(1, 0)$ as well. Second, on the upper surface $y = 0^+$ Woods' [16] approach is adopted for (2.1e), giving the relation

$$2\zeta_0 = -\zeta_2 - 6\psi_2/h^2 \tag{2.5}$$

between the unknown surface velocity and nearby streamfunction and vorticity values. With the analogous relation applied at the lower surface $y = 0^-$ also, two sets of ζ values along $y = 0$ are required to be stored/updated simultaneously, during the iteration procedure, to allow for the nonsymmetry in the vorticity values on either side of the plane. Next, the farfield conditions (2.1c) are replaced, at the outer boundaries, by rather simple constraints in the following way. At the boundary $x = x_{-\infty}$ for instance we take the Taylor series result

$$\psi_1 - \psi_3 = 2h(\partial\psi/\partial x)_0 + h^3(\partial^3\psi/\partial x^3)_0/3 + \mathrm{O}(h^5)\,, \tag{2.6}$$

with suffices $0 \to 4$ denoting the grid points $(x_{-\infty}, y)$, $(x_{-\infty} + h, y)$, $(x_{-\infty}, y + h)$, $(x_{-\infty} - h, y)$, $(x_{-\infty}, y - h)$ in turn, and combine this with (2.3) [applied with the same notation] to eliminate the extra-grid value ψ_3. Thus the requirement $(\partial\psi/\partial x)_0 = -\sin\alpha$ then leads to the expression

$$2\psi_1 + \psi_2 + \psi_4 - 4\psi_0 = -2h\sin\alpha - h^2\zeta_1/3 \tag{2.7}$$

after $(\partial^3\psi/\partial x^3)_0$ is replaced by $(-\partial\zeta/\partial x - \partial^3\psi/\partial y^2\partial x)_0$ from (2.1b), $\partial^3\psi/\partial y^2\partial x$ is set to zero

along $x = x_{-\infty}$, $(\partial\zeta/\partial x)_0$ is approximated by $(\zeta_1 - \zeta_0)/h$ [with little loss of accuracy in (2.6)] and ζ_0 is equated to zero. Here (2.7) is regarded as a formula for updating ψ_0 in the iterative procedure described below. Similar reasoning is applied to the edges $y = y_{\pm\infty}$, yielding

$$2\psi_2 + \psi_1 + \psi_3 - 4\psi_0 = 2h\cos\alpha - h^2\zeta_2/3 \tag{2.8}$$

along the edge $y = y_{-\infty}$ for example. At the fourth edge $x = x_\infty$ in contrast we decided to apply a boundary-layer exit condition like that in Smith and Dennis [12], which seems a fairly sensible step for small values of α at least. Bearing in mind the nonsymmetry of the flow and our emphasis on properties at the plate surface, as noted in Sec. 1, we chose to keep the outer constraints as described above, although many other representations are available and some may be investigated in further studies.

The finite-difference system above was solved by Gauss-Seidel sweeping, analogous to that of Dennis *et al.* [4, 6], Smith and Dennis [12] and others, from a given initial guess. Basically, each sweep consisted of updating, in order, the interior ζ distribution from (2.2) [amended for the two special points], the end $x_\infty - h$ values of ζ from the exit x_∞ conditions, then the outer $y_{\pm\infty}$ and $x_{-\infty}$ values of ψ from (2.7), (2.8), the interior ψ field from (2.3), the end $x_\infty - h$ values of ψ, and the plate vorticity distribution from (2.5). The outer vorticity values and the plate values of ψ were maintained at zero throughout, and some over-relaxation was applied occasionally in the use of (2.2), (2.3). The overall convergence criterion was based on the sum of the absolute changes in ζ being less than 0.0005 in successive sweeps.

Computational results, including the effects of the grid distribution, are presented below.

3. Numerical results

The main computed results obtained so far by the method of Sec. 2 are presented in Figs 2–4. These show plots of the calculated vorticity $\zeta_w^{\pm}$ on the plate surfaces, versus x, for three

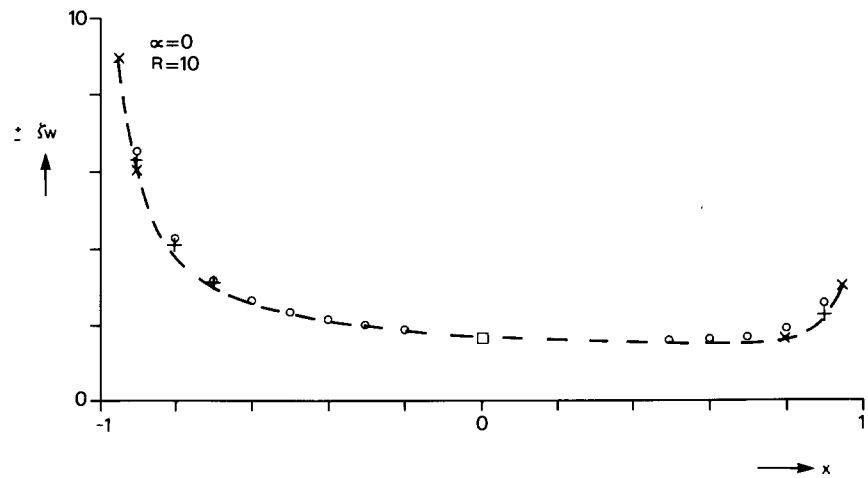

Fig. 2. Computed results for the wall shear stress ζ_w for the aligned plate $\alpha = 0$ at Reynolds number Re = 10: results 0, + give $\zeta_w^{\pm}$ from the grid $[x_{\pm\infty}, y_{\pm\infty}, h] = [4, 4, \frac{1}{10}]$; results – – –, × are from the grid $[4, 4, \frac{1}{20}]$. Also shown are sample values (□) from Dennis and Dunwoody [3], for comparison.

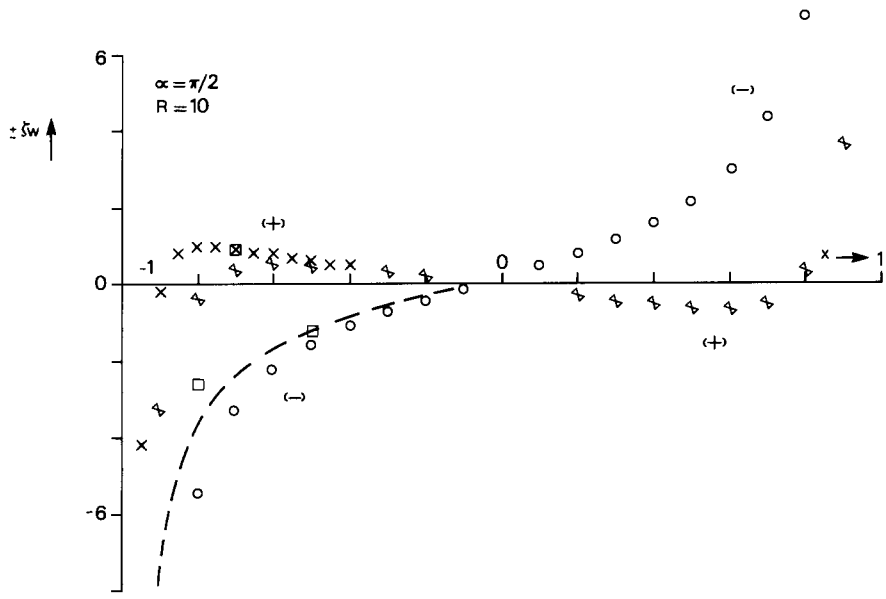

(a)

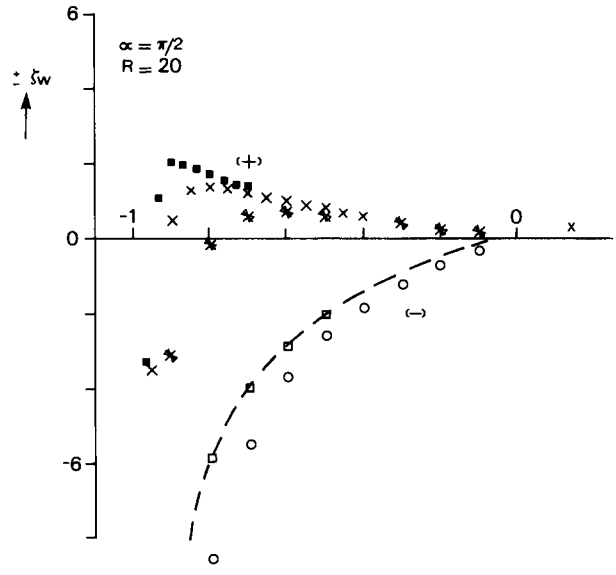

(b)

Fig. 3. Computed results for the normal flat plate $\alpha = \pi/2$, with ± sides as indicated. (a) Re = 10; 0, ↷ from grid $[4, 4, \frac{1}{10}]$; – – –, × from $[4, 4, \frac{1}{20}]$; for comparison, □ from Dennis and Hudson [7]. (b) Re = 20; 0, ↷ from $[8, 8, \frac{1}{10}]$; – – –, × from $[4, 4, \frac{1}{20}]$; □, ■ from $[4, 4, \frac{1}{30}]$. (c) Re = 50; – – –, × from $[4, 4, \frac{1}{20}]$.

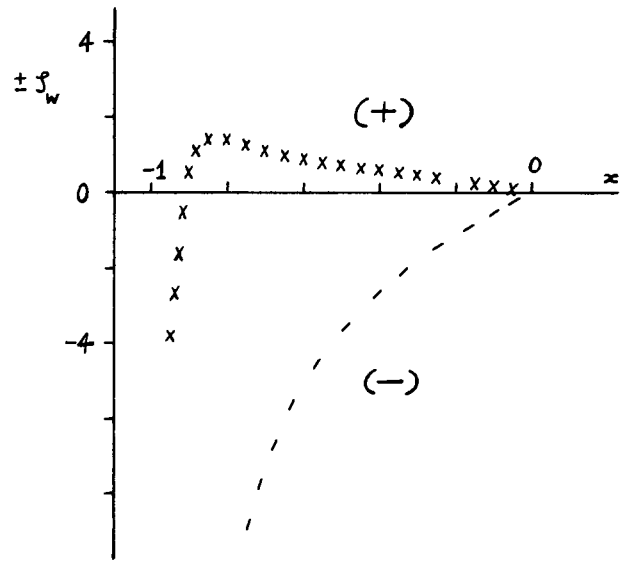

(c)

Fig. 3 (cont.)

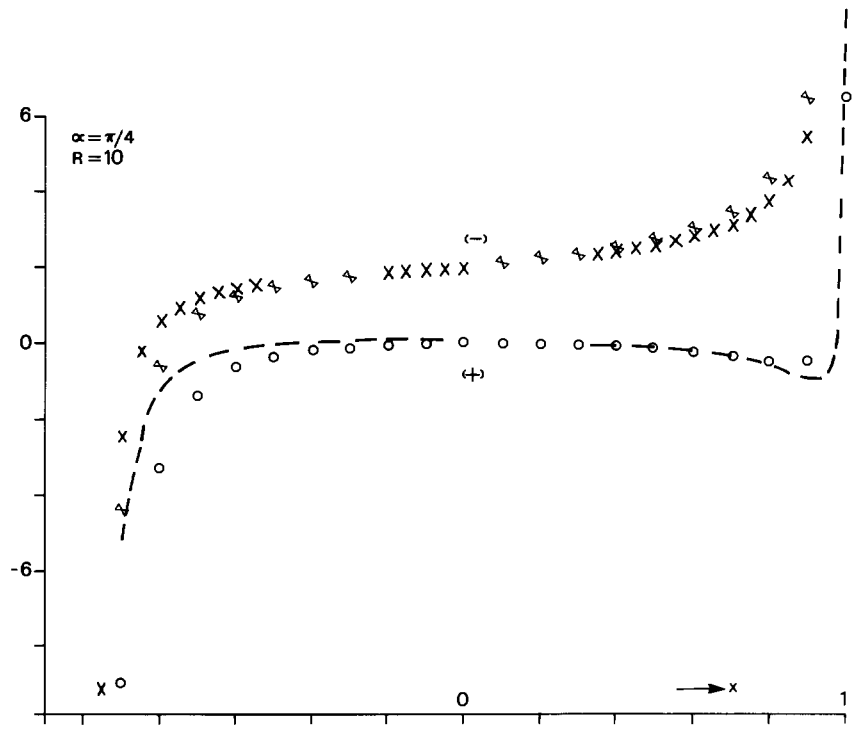

(a)

Fig. 4. Computed results for the inclined case $\alpha = \pi/4$, with ± sides as indicated. (a) Re = 10; 0, ⌔ from grid $[4, 4, \frac{1}{10}]$; – – –, × from $[4, 4, \frac{1}{20}]$. (b) Re = 20; 0, ⌔ from $[8, 8, \frac{1}{10}]$; – – –, × from $[4, 4, \frac{1}{20}]$; ●, ▲ from $[4, 4, \frac{1}{25}]$. (c) Re = 40; results a, b, c, d are from grids $[4, 4, \frac{1}{10}]$, $[8, 8, \frac{1}{10}]$, $[4, 4, \frac{1}{20}]$, $[4, 4, \frac{1}{25}]$ in turn.

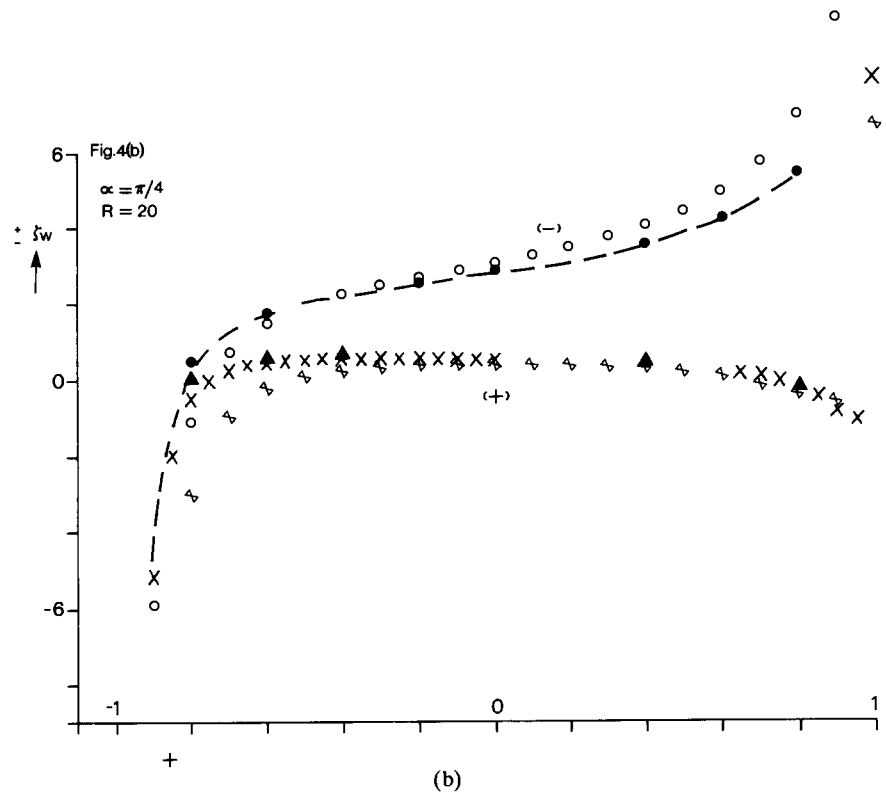

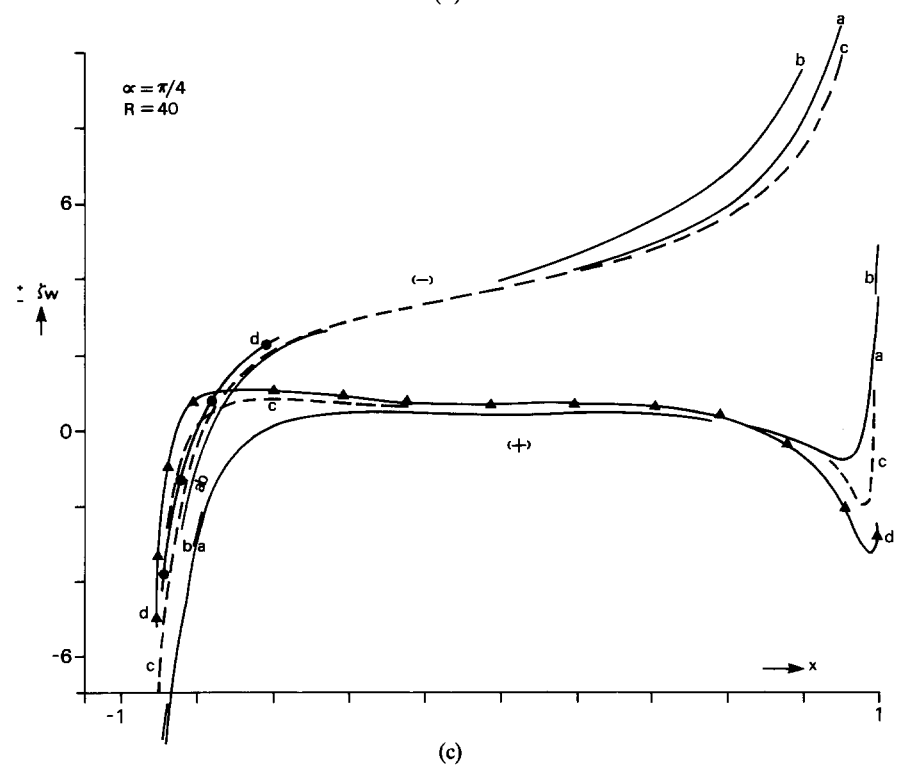

Fig. 4 (cont.)

angles of incidence α and various Reynolds numbers Re, with the superscripts $\pm$ here referring to the "upper" and "lower" plate surfaces $y = 0^{\pm}$ respectively. We show the plate-vorticity distribution in each partly because it is one of the most sensitive features of the calculations and partly because our concern is predominantly with the ability to determine surface properties, as mentioned in Sec. 1. The figures also give some comparisons with previous computations in the particular cases $\alpha = 0$, $\alpha = \pi/2$ and certain grid-effect studies.

Figure 2 shows the results for the aligned configuration $\alpha = 0$, when Re = 10. Here the method, which makes no assumption of symmetry, produces flow solutions which are virtually symmetric in y, as might be expected at the Reynolds number concerned. A comparison is made with the Dennis and Dunwoody [3] solution at Re = 10 and this proves favourable on the whole. Comparisons of the results from different grids are also shown, suggesting that the grids used are reasonably adequate in this case.

In Fig. 3(a–c) we move on to the other special case, that of the broadside-on flat plate where $\alpha = \pi/2$. Again almost symmetrical solutions for the plate vorticity are produced (the symmetry being with respect to x) despite, in this case, the nonsymmetry of the treatment of the farfield conditions as discussed in Sec. 2. The computations shown here are for Re = 10, 20, 50 and a comparison is made with Hudson and Dennis' [7] results at the highest Reynolds number of their calculations, Re = 10. The agreement is fairly close overall, the more so if h^2-extrapolation is performed on our results, as Fig. 3(a) shows. There is one peculiar feature to stress, however. It is that for each particular grid taken, the plate vorticity on the "+" (downstream) surface near the edges of the plate rapidly passes through zero and changes sign, compared with the more gradual development over the rest of that surface. This phenomenon we may ascribe to a distorting influence from the geometrical treatment of the local singularity, especially since grid refinement consistently reduces or delays the phenomenon and gradually pushes the local solution more towards the opposite singular-like behaviour that is to be expected. It may well be that the above phenomenon of sudden crossing in the plate vorticity occurs as a result of the local geometrical method linking together too closely the vorticity values around the salient edge, which, in view of the accelerating flow streaming from the "−" side, causes an unrealistically large overspill numerically onto the "+" side. Grid refinement serves to counteract and diminish this feature, however, as we have mentioned. Grid-effect studies are shown in both of the Figs 3(a, b), we note further, but not in 3(c), at the largest Re, the results for which should therefore be regarded as the most tentative of the calculations.

Finally here, Fig. 4(a–c) presents the results obtained for the inclined case $\alpha = \pi/4$, when Re = 10, 20, 40. The effects of the grid distribution are demonstrated at each Reynolds number and they are broadly similar to those above for $\alpha = \pi/2$, although with regard to the changes in the responses close to the salient edges $x = \pm 1$ the local sensitivity there appears to be much reduced for $\alpha = \pi/4$. The patterns of these nonsymmetric results for the surface vorticity distributions almost certainly indicate the formation of two counter-rotating eddies of unequal sizes on the downstream side, as would be expected physically, although an alternative formation (for small α values at least) is that of a single eddy downstream. The patterns, and the existence of the reattachment point where $\zeta w^+ = 0$ on the top surface, are in line with the asymptotic theory of Smith [10] and the interactive boundary-layer computations of Vatsa and Verdon [14] for nonsymmetric airfoil flow.

We should also note that the case of the normal flat plate ($\alpha = \pi/2$) seems to be one of the most difficult computational problems. Hudson and Dennis [7] found difficulty in

obtaining accurate solutions beyond Re = 10 and in more recent work (Dennis and Wang Quang, to be published) it has been found difficult to proceed beyond Re = 35. In both cases elliptic coordinates were used so that the calculations are not easily comparable with the present work, but Dennis and Wang Qiang found that a grid size of 1/100 of the plate length was necessary for Re = 35. The results obtained by the present method for this difficult case seem therefore to be reasonable, having regard to the cautions mentioned above.

4. Further comments

The computational results presented in the previous section for flow past inclined plates, along with the comparisons and checks there, suggest to us that overall the relatively simple method used in this work for handling the salient edges could be of some further value, in nonsymmetric airfoil-flow computations for instance. The singularities at the edges, combined with our particular numerical treatment near them, certainly produce some distortions in the flow solutions, more so than in our earlier study [12], but these do appear to be quite localized phenomena in the main. Extra grid refinement and/or grid stretching may well alleviate the local problems further, when combined with the present treatment; or perhaps a more satisfactory treatment of the singularities would improve the situation.

Whether the distorting effects above continue to be localized or not at higher Reynolds numbers and at other angles of incidence remains to be seen, as does the influence of the outer boundary conditions used in the present work. Converged results have not been obtained yet at higher Reynolds numbers for the angles $\alpha = \pi/2$, $\pi/4$ of Figs 3, 4 but we might anticipate that the accurate prediction of leading-edge and trailing-edge separation/stall will be less difficult at smaller α values. Moreover, the results so far seem to be not inconsistent with the trends predicted by asymptotic and approximate theories based on small incidence angles α as noted in Sec. 3. Further computational studies of the nonsymmetric motions, along these lines, could be of much interest, we feel.

Thanks are due to the S.E.R.C., U.K., for providing the computer facilities for F.T.S. at Daresbury and at the University of London Computing Centre and to the Royal Society for financial support for S.C.R.D. on a Guest Research Fellowship at University College.

References

1. Dennis, S.C.R., Finite differences associated with second-order differential equations, *Quart. J. Mech. Appl. Math.* 13 (1960) 487–507.
2. Dennis, S.C.R., Calculations referred to in Stewartson, K., 1974, Multi-structured boundary layers on flat plates and related bodies, *Advs. in Appl. Mechs.* 14 (1974) 145–239.
3. Dennis, S.C.R. and Dunwoody, J., The steady flow of a viscous fluid past a flat plate, *J. Fluid Mech.* 24 (1966) 577–595.
4. Dennis, S.C.R. and Hudson, J.D., A difference method for solving the Navier-Stokes equations, *Proc. 1st Int. Conf. on Num. Meths. in Lam. and Turb. Flow*, Pentech Press (1978) 69–80.
5. Dennis, S.C.R. and Hudson, J.D., Compact h^4 finite-difference approximations to operators of Navier-Stokes type, *J. Computational Phys.* 85 (1989) 390–416.
6. Dennis, S.C.R. and Smith, F.T., Steady flow through a channel with a symmetrical constriction in the form of a step, *Proc. Roy. Soc. A* 372 (1980) 393–414.
7. Hudson, J.D. and Dennis, S.C.R., The flow of a viscous incompressible fluid past a normal flat plate at low and intermediate Reynolds numbers: the wake, *J. Fluid Mech.* 160 (1985) 369–383.

8. Jobe, C.E. and Burggraf, O.R., The numerical solution of the asymptotic equations of trailing edge flow, *Proc. Roy. Soc. A* 340 (1974) 91–111.
9. Mehta, U.B., in *Unsteady Aerodynamics*, AGARD Conf. Proc. CP-227, paper 23 (1977).
10. Smith, F.T., Interacting-flow theory and trailing-edge separation – no stall, *J. Fluid Mech.* 131 (1983) 219–249, and U.T.R.C. Rept. UT82-13.
11. Smith. F.T., Steady and unsteady boundary-layer separation, *Ann. Rev. Fluid Mech.* 18 (1986) 197–220.
12. Smith, F.T. and Dennis, S.C.R., Injection from a finite section of a flat plate placed parallel to a uniform stream, *J. Eng. Math.* 15 (1981) 267–286.
13. Stewartson, K., Smith, F.T. and Kaups, K., Marginal separation, *Stud. in Applied Math.* 67 (1982) 45–61.
14. Vatsa, V.N. and Verdon, J.M., Viscid-inviscid interaction analysis of separated trailing-edge flows, *A.I.A.A. Jnl.* 23 (1985) 481–489.
15. Veldman, A.E.P. and Van de Vooren, A.I., Proc. 4th Int. Conf. on Num. Meths. in Fluid Dyn., *Lecture Notes in Physics*, Springer 35 (1974) 423–430.
16. Woods, L.C., A note on the numerical solution of fourth order differential equations, *Aero. Quart.* 5 (1954) 176–184.